

## Supporting Information

### **Mushroom-mimetic 3D hierarchical architecture-based e-skin with high sensitivity and wide sensing range for intelligent perception**

*Yajie Zhang, Xinyu Zhang, Chuan Ning, Kun Dai, Guoqiang Zheng,\* Chuntai Liu, Changyu Shen*

College of Materials Science and Engineering, National Engineering Research Center for Advanced Polymer Processing Technology, Zhengzhou University, Zhengzhou 450001, PR China

E-mail addresses: gqzheng@zzu.edu.cn (G. Zheng).

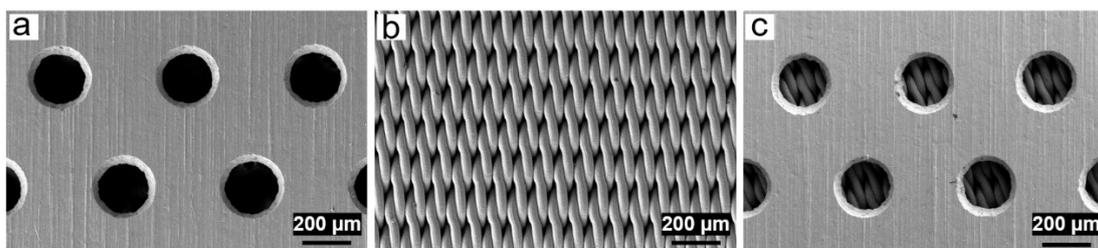


**Fig. S1.** SEM images of (a) punched plate, (b) mesh sieve and (c) punched plate stacked with mesh sieve.

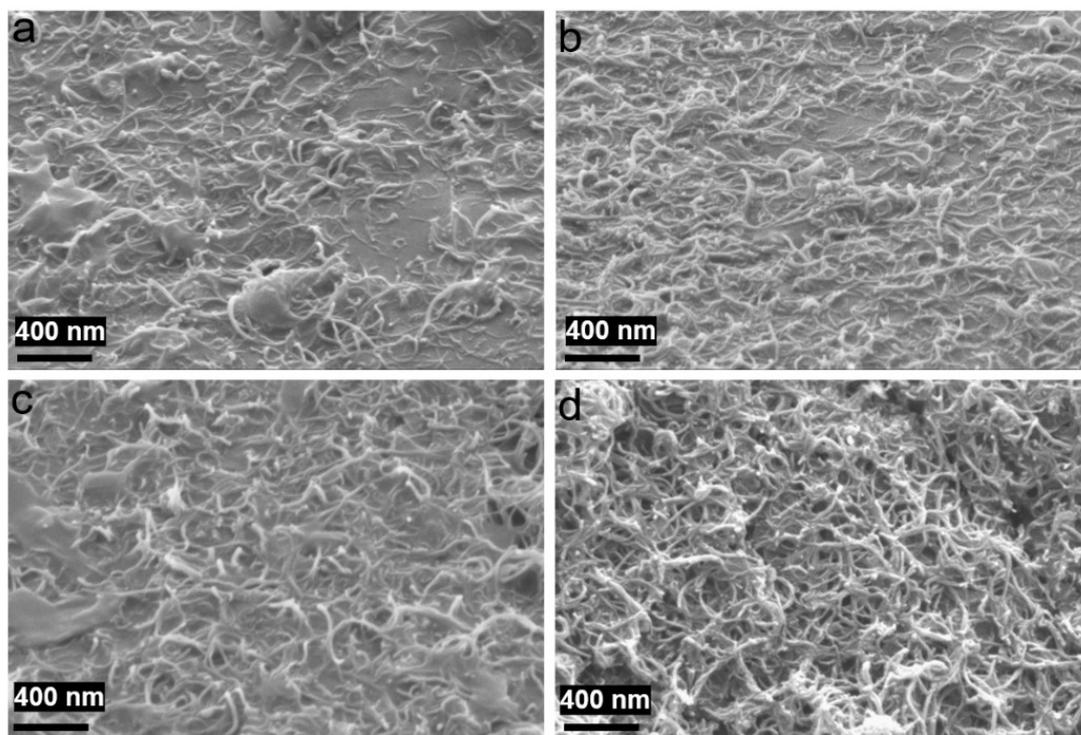


**Fig. S2.** SEM images of CNTs networks on the surface of MMTC sprayed for (a) 4, (b) 5, (c) 6 and (d) 7 times.

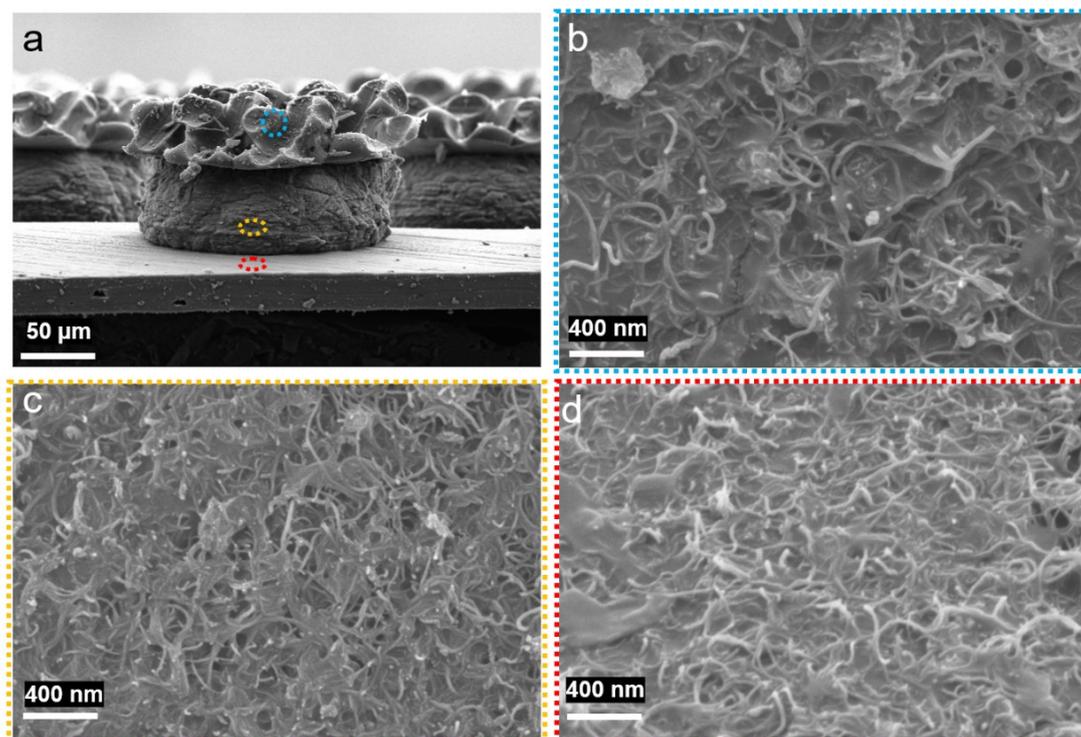


**Fig. S3.** (a) Side view SEM images of MMTc sprayed for 6 times. SEM images of CNTs networks on (b) top, (c) side wall and (d) bottom of micropattern.

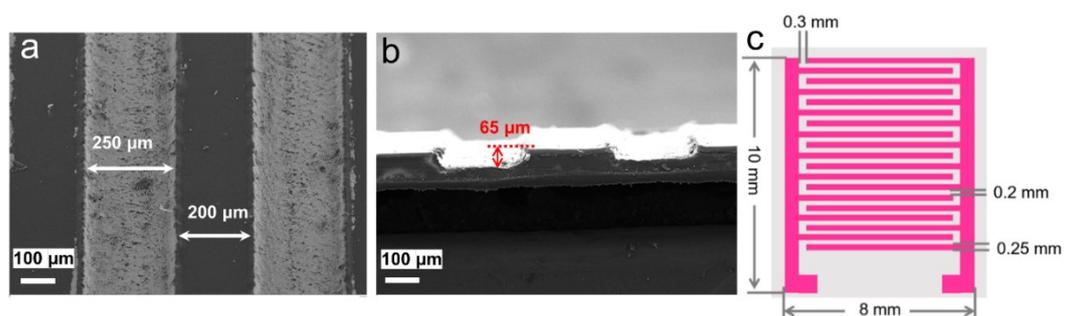


**Fig. S4.** The dimensions of the interdigital electrode.

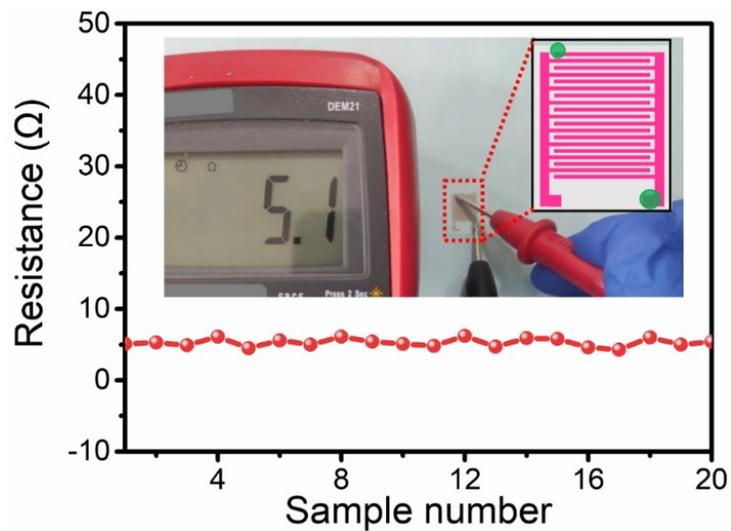


**Fig. S5.** The linear resistance per centimeter of as-prepared interdigital electrode.

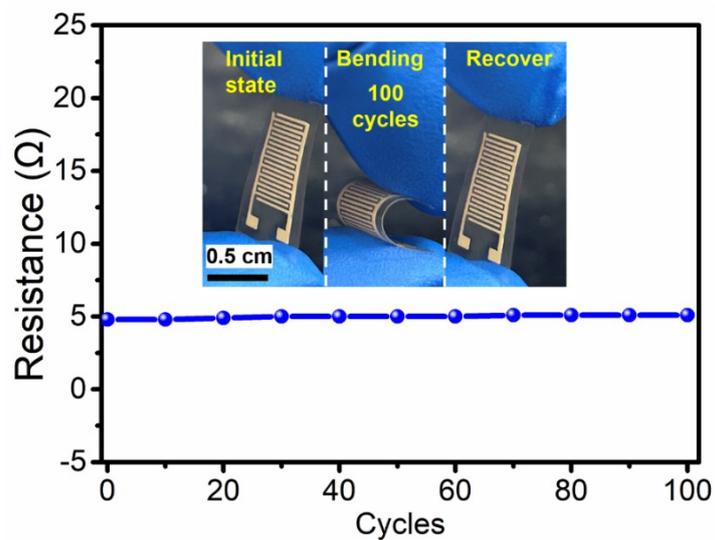


**Fig. S6.** The linear resistance per centimeter of interdigital electrode after 100 cycles bending/recovery test.

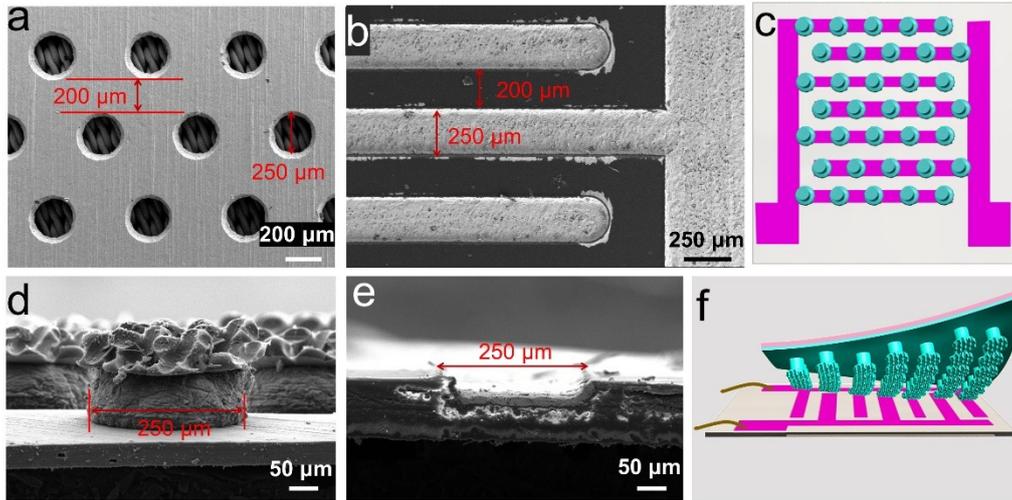


**Fig. S7.** (a) SEM images of punched plate stacked with mesh sieve. (b) Top view SEM images of the as-prepared interdigital electrode. (c) A diagram showing the distribution of mushroom-mimetic micropatterns on the as-prepared interdigital electrode. (d) Side view SEM images of MMTC. (e) Cross sectional view SEM image of the as-prepared interdigital electrode. (f) Schematic diagram of the structure of MMTC/interdigital electrode e-skin.

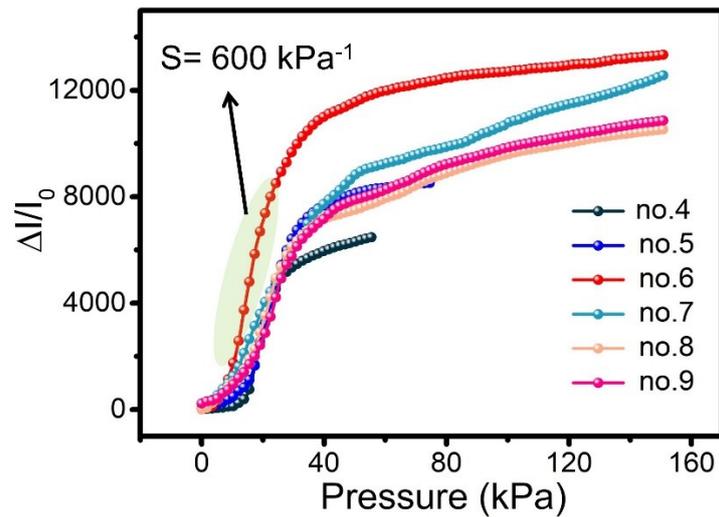


**Fig. S8.** Sensitivity of MMTC/interdigital electrode e-skins based on MMTC sprayed with CNTs dispersion for different times.

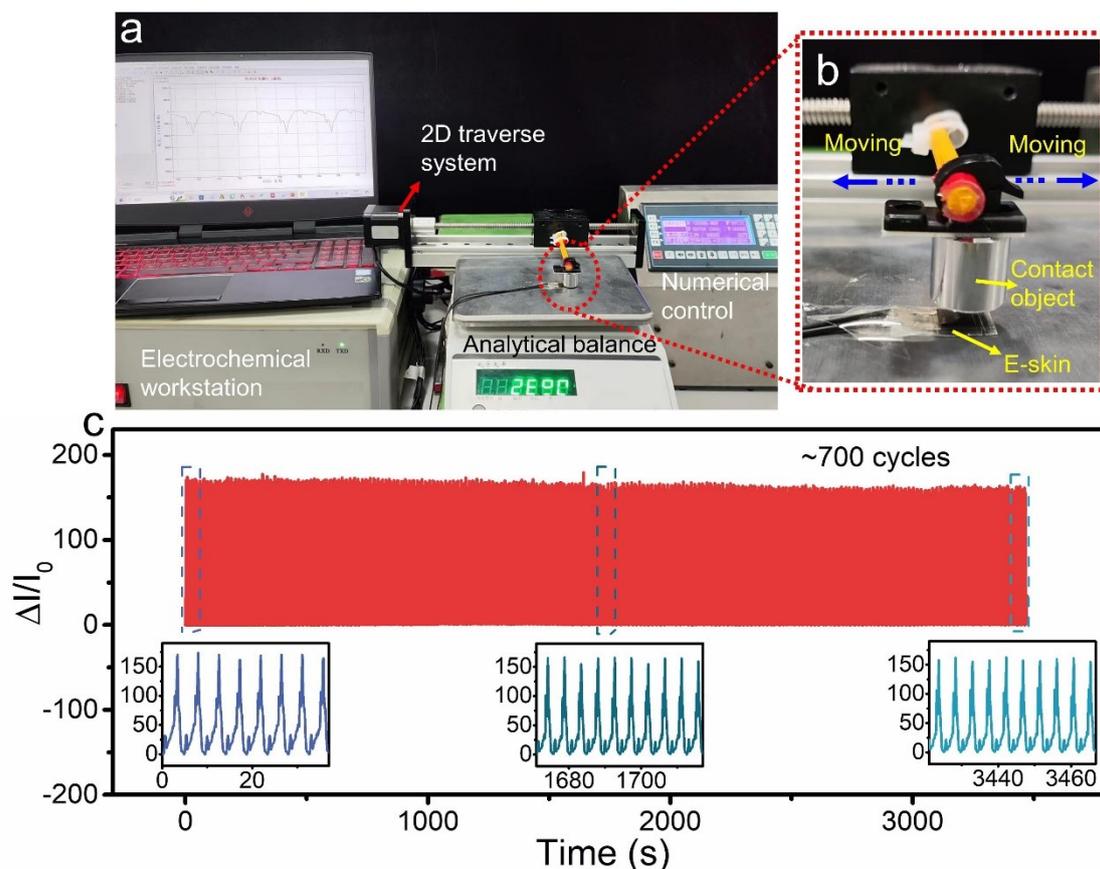


**Fig. S9.** (a, b) Picture of the home-made shear test equipment. (c) The e-skin was subjected to shear at a loading of 0.22 N for 700 cycles.

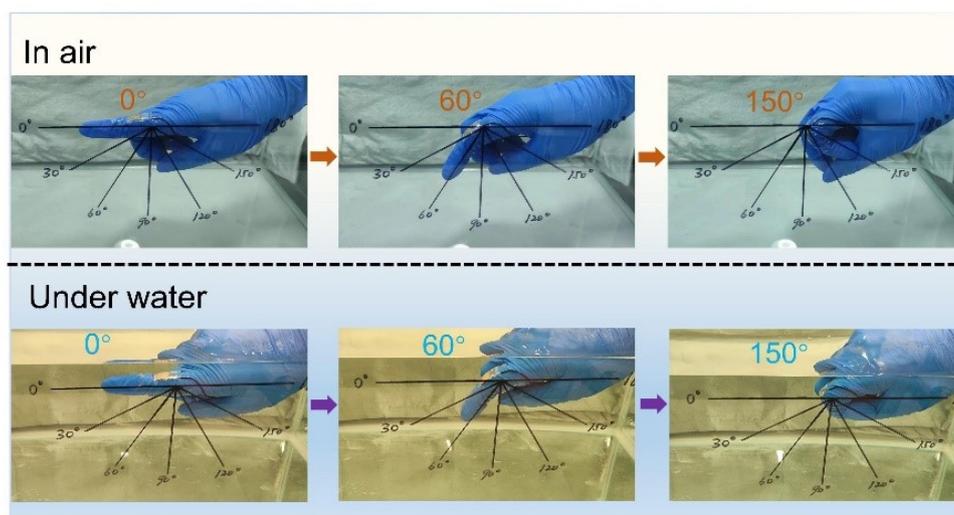


**Fig. S10.** Digital images displaying the index finger bending to different angles in air and under water. MMTC/interdigital electrode e-skin was simply packaged and attached on index finger bending to different angles in air or under water.

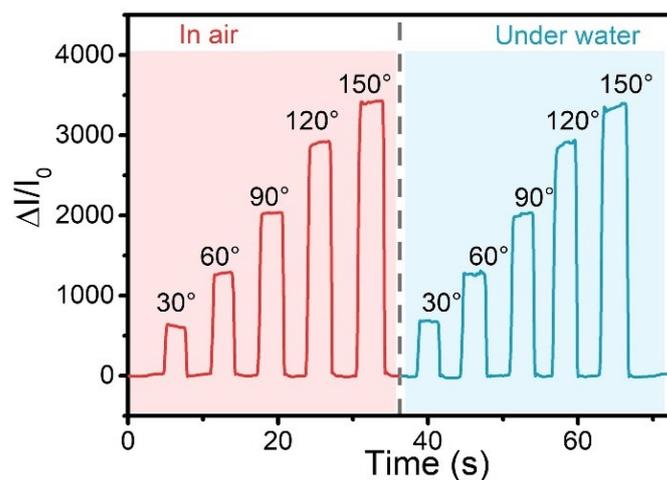


**Fig. S11.** Response of the index finger bending to different angles (from 30° to 150°) both in air (left side) and under water (right side).



**Fig. S12.** (a, b) Schematic diagram of underwater communication based on the principle of Morse code.

<b>Mechanism</b>	<b>Sensitivity (kPa<sup>-1</sup>)</b>	<b>Maximum sensing range(kPa)</b>	<b>Detection limit (Pa)</b>	<b>Response time (ms)</b>	<b>Cycles</b>	<b>Reference</b>
Pizoresistive	442	18.56	9	138	10000	<a href="#">41</a>
Pizoresistive	151.4	15	4.4	125	10000	<a href="#">42</a>
Pizoresistive	509.8	20	1	67.3	10000	<a href="#">43</a>
Pizoresistive	99.5	4.5	9	4	10000	<a href="#">44</a>
Pizoresistive	403.46	10	0.88	105.3	12000	<a href="#">45</a>
Pizoresistive	649.3	20.55	4	123	10000	<a href="#">46</a>
Pizoresistive	196	100	0.5	26	10000	<a href="#">47</a>
Pizoresistive	191.3	60	8	80	18000	<a href="#">48</a>
Pizoresistive	298.4	39.3	7.1	7	10000	<a href="#">49</a>
<b>Pizoresistive</b>	<b>600</b>	<b>150</b>	<b>5</b>	<b>20</b>	<b>15000</b>	<b><a href="#">This work</a></b>

**Table S1.** Performance comparison of different e-skins.